

Magnetic Modulation Biosensing for Rapid and Homogeneous Detection of Biological Targets at Low Concentrations

Amos Danielli^{1,*}, Noga Porat², Marcelo Ehrlich³ and Ady Arie¹

¹Department of Physical Electronics, Faculty of Engineering, Tel-Aviv University, Tel-Aviv 69978, Israel; ²Department of Biological Science, University of Illinois at Chicago, Chicago IL 60607, USA; ³Department of Cell Research and Immunology, Tel-Aviv University, Tel-Aviv 69978, Israel

Abstract: This paper reviews the development of a magnetic modulation biosensing (MMB) system for rapid, simple and sensitive detection of biological targets in homogeneous solution at low concentrations. It relies on condensation and modulation of the fluorescent-labeled probes attached to magnetic beads using an alternating magnetic field gradient. Condensation of the beads from the entire volume increases the signal while modulation separates the signal from the background noise of the non-magnetized solution. We first discuss the motivation and challenges in specific DNA sequences detection as well as current approaches to overcome some of these challenges. We then present the MMB system, DNA detection schemes and magnetic beads manipulation in solution. Rapid detection at sub-picomolar concentrations of fluorescent-labeled probes as well as of coding sequences of the non-structural Ibaraki virus protein 3 (NS3) complementary DNA (cDNA) without any washing or separation step is also reviewed. Finally, we show preliminary results of protein detection using a 'sandwich'-based assay.

Keywords: Ibaraki virus, DNA detection, Magnetic modulation, Magnetic beads, Fluorescence and luminescence, Magnetic nanoparticles, FRET.

1. INTRODUCTION

Rapid and sensitive detection of fluorescent-labeled probes at low concentrations is a well known challenge in many biological applications. Fluorescent-labeled biosensors are widely used in detection of specific DNA sequences and in protein-protein interactions [1]. Quickly obtaining a reliable result in conditions where a limited amount of genetic material is available is particularly challenging in face of the need to discern amongst different sequences, presenting minor alterations that may potentially lead to vastly diverging biological responses. For example, pathogens such as anthrax (*Bacillus anthracis*) are associated with changes in the sequence of particular genes. These changes can serve as biomarkers and may be useful for routine monitoring and genetic testing of environmental samples for early detection and response in the event of bioterrorist attack [2].

In general, a specific DNA sequence detection system combines two elements: (a) a biosensor that couples a biological recognition element, the bioreceptor (e.g. enzymes, oligonucleotide); with a physical transducer that translates the biorecognition event into an analytical signal (e.g. fluorescent dye, quantum dot, gold nanoparticles etc.) (b) a detection system that is sensitive enough to detect the physical signal (e.g. an optical system detects the fluorescent signal; an electrical system detects changes of conductivity etc.) [3]. The two most commonly used physical transducers are fluorescent labels and nanoparticles labels [4]. Fluorescent labels

offer high sensitivity and great diversity of fluorophores, while nanoparticles labels offer low cost, stability and unique physical-chemical properties. Ideally, DNA detection systems should combine high sensitivity, high speed (real-time measurements), simple operation and low production cost.

When marking the target analyte (e.g. DNA sequence) with a fluorescent probe, at low concentrations, the fluorescent signal is very weak and surrounded with background noise from the solution. There are two types of background photons: elastic Rayleigh/Mie scattering of the pump laser (at the same wavelength as the excitation laser) and photons that are red shifted in wavelength into the spectral region where fluorescence is detected. While Rayleigh/Mie-scattered pump radiation can be reduced using interference filters, red shifted photons, such as Raman scattering of the solvent and residual fluorescence from other impurities [5, 6], are more challenging to overcome. Both Raman scattering and residual fluorescence are proportional to the volume of the illuminated sample. Although the fluorescent yield of Raman scattering is very weak, unwanted impurities or molecules of the host medium (e.g. water molecules) can still emit strong residual fluorescence simply due to the fact that trillions of host molecules may be present in the illuminated volume.

Conventional genomic DNA (or RNA) detection methods mostly rely on polymerase chain reaction (PCR), a very sensitive detection method as it amplifies small quantities of genetic material and has been employed in the detection of the presence of bacteria. However, it is costly, requires hours of processing and expertise in molecular biology [7]. Hence, it is difficult to use it in real time measurements. Alternatively, DNA sequences can be directly detected from unam-

*Address correspondence to this author at the Department of Biomedical Engineering, Washington University in St. Louis, Tel: (314) 9359587, Fax: (314) 9357448, One Brookings Drive, Box 1097, St. Louis, 63146, MO, USA; E-mail: amosd@post.tau.ac.il

plified genomic DNA, e.g. by using fluorescent-labeled probes. One approach uses direct detection of the fluorescent light. To improve sensitivity, long (more than one hour) non-PCR amplification methods are required (e.g. using rolling circle amplification [8] or serial invasive signal amplification reaction [9]). Another approach also uses fluorescent-labeled probes but improves the sensitivity using time-resolved fluorescence detection. These methods to detect low concentrations of fluorescent dyes in solution are based on single molecule burst detection techniques. Single molecule detection in solution is mainly based on the use of confocal fluorescent spectroscopy, which detects the emission from a single fluorescent molecule when it passes through a femtoliter-size detection volume. The small detection volume reduces the background noise originating from Raman scattering of solvent molecules or residual fluorescence from other impurities. For example, Castro *et al.* (1997) utilized time-correlated single photon counting (TCSPC) and two-color fluorescent coincidence analysis to detect specific nucleic acid sequences in unamplified genomic DNA [10]. One of the advantages of pulse excitation (i.e. TCSPC) is the ability to utilize time gated detection. The detection electronics rejects prompt Raman and Rayleigh scattering by using a time-gate window set such that only delayed fluorescence photons are detected, thus increasing the signal-to-noise ratio of the single molecule detection. Wabuyele *et al.* (2003) demonstrated a rapid detection scheme capable of detecting rare point mutation in unamplified genomic DNA using single-molecule fluorescent burst detection [11]. Foldes-Papp *et al.* (2005) demonstrated direct probing of unamplified genomic DNA in solution down to femtomolar allele concentrations using two-color fluorescence cross-correlation spectroscopy [12].

A third approach to detect low concentrations of DNA uses metallic or semiconductor nanoparticles for biosensing and a detection system that is either electrical [13], optical [14-16] or magnetic [17]. Fluorescent semiconductor nanoparticles (quantum dots) offer superb photophysical properties compared to organic dyes: strong extinction coefficient, increased stability to photobleaching, a narrow emission peak and lack of long 'red tail', which causes cross-talk in multicolor fluorescent experiments, all of which make them excellent candidates to be used as fluorescent tags [18, 19]. Several methods have been developed based on scatter light from gold nanoparticles. Nam *et al.* (2004) have developed a Bio-Bar-Code based DNA detection which is capable of detecting short oligonucleotide targets at attomolar concentrations. However, the entire assay is carried out within 3-4 hours [16]. Storhoff *et al.* (2005) demonstrated detection of approximately 20,000 copies of genomic DNA target in 1- μ l volume within 2 hours [14]. Bao *et al.* (2005) demonstrated detection of single nucleotide polymorphisms (SNPs) with 150,000 genome copies in 5 μ l of human genomic DNA [15]. While time-resolved fluorescent measurements and nanoparticles-based techniques usually offer higher sensitivity and faster results, the required analysis time may still be relatively long. Moreover, some of these methods require washing and separation steps that complicate the detection process.

Recently, we experimentally demonstrated a novel biosensing method that aims to overcome these drawbacks [20,

21]. It relies on condensation and modulation of the fluorescent-labeled probes that are coupled to magnetic beads using an external magnetic field gradient. The method offers high sensitivity, since the magnetic field attracts the fluorescent-labeled probes from the entire solution volume into a small detection area. Furthermore, the modulation of the magnetic beads (coupled to fluorescent-labeled probes) enables separation of the signal from the background noise of the non-magnetized solution. Narrowing the detection bandwidth eliminates most of the noise and provides significant improvement in the measurement sensitivity. Moreover, condensation and modulation of the magnetic beads eliminates the need for separation and washing steps usually incorporated in heterogeneous assays, thereby shortening and facilitating the detection assay. The most common use of magnetic beads in DNA detection is for separation and purification of probe hybridization [22]. A magnet is attached to the container wall of a solution of magnetically tagged biomaterials. The tagged particles are gathered by the magnet, and the unwanted supernatant solution is removed. In another application, magnetic microspheres act as the surface for initial immobilization of the target material and magnetic separation is used to increase the concentration of the material [22]. Magnetic modulation has also been used either to rotate or maneuver magnetic beads in order to increase signal to noise ratio [23, 24]. Anker *et al.* (2003) developed magnetically modulated optical nanoprobe that blink in response to rotating magnetic fields [24-26]. By separating the blinking probe signal from the unmodulated background, they can sensitively detect low chemical concentrations even in the presence of autofluorescence and other backgrounds. These probes are fluorescent polystyrene microspheres containing ferromagnetic material. One hemisphere of the particles is coated with opaque metal layer while the other hemisphere is labeled with fluorescent dye. The particle is then magnetized so that the uncoated light-emitting side is the magnetic north of the particle. The particles were mainly used as orientation and torque sensors as well as to improve measurements inside cells [25]. Nevertheless, rapid, sensitive and homogeneous detection of specific DNA sequences using magnetic modulation of magnetic beads without separation steps has never been demonstrated.

In this paper we will review the magnetic modulation biosensing (MMB) system and its applications. We first demonstrated the high sensitivity of the MMB technique by detecting fluorescent-labeled oligonucleotides at 30 fM concentration. Later, we utilized a novel fluorescence resonance energy transfer (FRET)-based probe and applied the MMB system, which simply (no separation steps), rapidly (<18 min) and sensitively detected the coding sequence for the non structural Ibaraki virus protein 3 (NS3). The advantages of MMB due to condensation and modulation were evident by comparing the system results to measurements obtained by a laser scanning microscope and a standard real-time PCR (i.e. RT-PCR) assay. Finally, we show preliminary results of protein detection using a 'sandwich'-based assay without any separation or washing step.

2. DNA BIOSENSORS

In general, any approach which as a result of the biorecognition event produces fluorescent light (e.g. FRET-based

assay [27]) or connects a magnetic bead to a fluorescent dye (e.g. 'sandwich'-based assay [3,28]); can utilize the MMB system to detect low concentration of labeled probes. A novel FRET-based synchronous detection assay is illustrated in Fig. (1a). A short nucleic acid probe is double-labeled with a fluorescent dye (donor) and biotin on the same nucleotide at the 5' end. A dark quencher is connected at the 3' end. During PCR, the discriminating FRET-based probe will hybridize with its complementary nucleotide sequence (i.e. detection of specific DNA sequence has been made). Similar to RT-PCR reaction with Taqman® probes [29], during the extension phase of the PCR, the 5'-3' exonuclease activity of the *Taq* polymerase cleaves the fluorescent label (still attached to the biotin) from the probe and upon excitation with a laser beam, fluorescent light is produced. Conversely, if the discriminating probe is not complementary to the target DNA, the probe remains intact and the fluorescent labeled nucleotide remains quenched by the dark quencher. An alternative to the FRET-based approach involves a three-component 'sandwich' assay, in which the label is associated with a third DNA sequence (the signaling probe) designed to be complementary to an overhanging portion of the target. This dual hybridization increases the specificity of the detection. A suggested 'sandwich'-based synchronous detection assay is illustrated in Fig. (1b). A single-stranded DNA (ssDNA) called the 'capture probe' is labeled with biotin at the 5' end. Another ssDNA, called the 'signaling probe' is labeled with a fluorescent dye (or quantum dot) at the 3' end. If detection is made; the two probes hybridize to the complementary target DNA. Thus, the fluorescent dye can be connected to streptavidin-coupled magnetic beads via the

biotin. Each magnetic bead can be attached to thousands of fluorescent labeled probes and set in a 1-D periodic motion. Conversely, if the discriminating probes are not connected to the target DNA, than the magnetic particle is not connected to the fluorescent dye and magnetic modulation will not yield a synchronous fluorescent signal. One of the main advantages of the 'sandwich'-based assay over the FRET-based assay is the fact that there is no residual fluorescence when the target is not presence.

3. MAGNETIC MODULATION BIOSENSING SYSTEM

A magnetic particle in a field is subject to mechanical forces of magnetic origin due to the interplay between its magnetic moment \vec{m}_B and the external field \vec{B} . A torque $\vec{\tau} = \vec{m}_B \times \vec{B}$ will tend to rotate and align the particle's moment with the external field. If the field is not constant and presents a gradient $\vec{\nabla}B$, the particle is subject to a force proportional to the local field gradient:

$$\vec{F}_m = \vec{m}_B \cdot (\vec{\nabla}B) \quad (1)$$

The force is directed toward the regions of higher magnetic field. While magnetic particles can consequently be pulled in the direction of increasing fields, they can never be pushed away [30]. In order to manipulate magnetic beads in a 1-D synchronous motion, at least two magnetic poles, as well as the use of nonpermanent field, need to be implemented in the system [31]. High forces on relatively small magnetic beads require proper bead material (i.e. high mag-

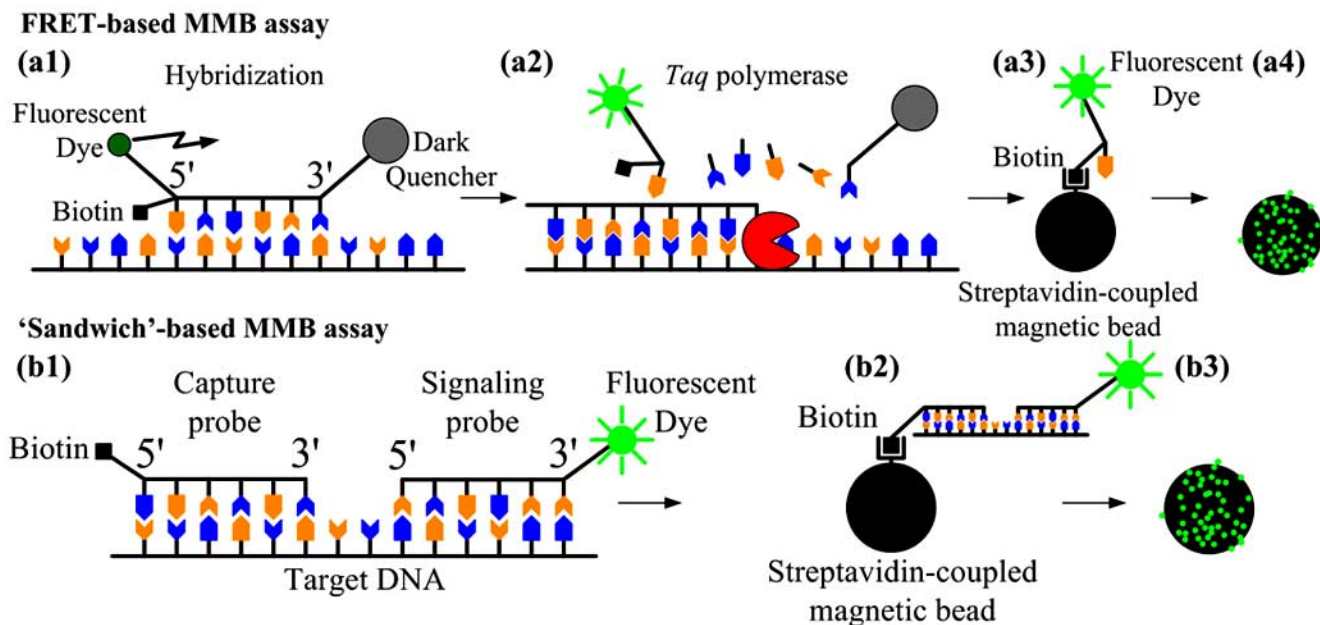


Fig. (1): (a) Illustration of the FRET-based MMB assay: (a1) A nucleic acid probe is double-labeled with a fluorescent dye and biotin at the 5' end on the same nucleotide and a dark quencher at the 3' end. (a2) When detection occurs, each cycle of PCR separates the fluorescent dye from the dark quencher and fluorescent light is produced upon light excitation. (a3) The fluorescent dyes are connected via the biotin to streptavidin-coupled magnetic beads. (a4) Each magnetic bead can be attached to thousands of fluorescent labeled probes and can be set in 1-D periodic motion; (b) Illustration of the 'sandwich'-based MMB assay: (b1) a capture probe, labeled with biotin at the 5' end and a signaling probe, labeled with a fluorescent dye at the 3' end, hybridize to the complementary target DNA. (b2) If hybridization is made, the fluorescent dyes are connected via the biotin to streptavidin-coupled magnetic beads. (b3) Each magnetic bead can be attached to thousands of fluorescent labeled probes and set in a 1-D periodic motion.

netic moment) and optimization of field gradient. The maximum achievable field gradient depends on both the saturation magnetization of the pole material and the geometry of the pole tips. Parabolic-shaped pole tip provides higher field gradient than a flat-top pole tip at a predefined distance from the pole tip [20].

In general, the novel MMB system utilizes Streptavidin-coupled magnetic beads that are attached to the biotinylated probes. Two external electromagnetic poles condense the magnetic beads into the detection area and set them in a 1-D periodic motion by modulating the magnetic field gradient. This periodic motion, in and out of an orthogonal laser beam, produces a periodic fluorescent light, which is collected by a photomultiplier (PMT) and demodulated using a lock-in amplifier (see Fig. (2)). A comprehensive description of the system set-up as well as the magnetic pole fabrication can be found in previous papers [20,21].

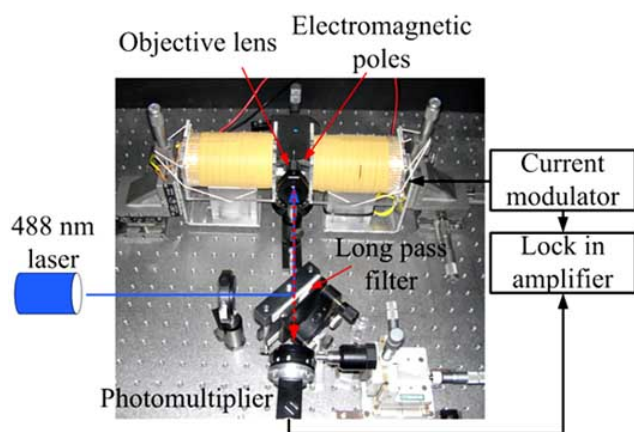


Fig. (2). Experimental set-up of the magnetic modulation biosensing system.

In order to maneuver the magnetic beads in a periodic 1-D movement we used a homemade current modulator. The current modulator produced successively to each coil a square-wave with amplitude of 1.4 A at a chosen frequency in the range of 1-6 Hz. If each pole is active at 1 Hz, the beads enter and leave the laser beam twice (see Fig. (3)), yielding a signal at 2 Hz. Thus the modulation frequency at the lock-in amplifier was between 2-12 Hz.

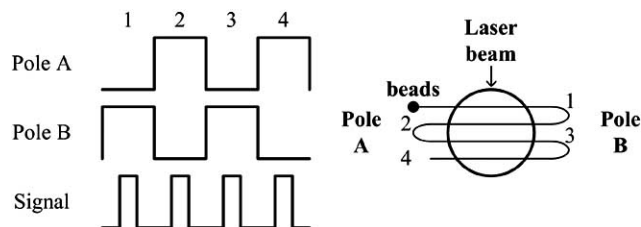


Fig. (3). Current modulation frequency of the poles is half the frequency of the expected signal.

We tested our MMB system using 2.8 μm diameter streptavidin-coupled superparamagnetic beads (Dynabeads, M-280, Invitrogen), which according to the manufacturer [32] have volume magnetization of 14,000 A/m and density of

1400 kg/m^3 . Due to high magnetic forces applied by the poles, it was difficult to place the poles too close to the cuvette's walls. The poles attracted each other and caused the setup to vibrate. Therefore, the poles were positioned at a distance of ~ 4 mm from each other (~ 2 mm from the center of the cuvette). The following calculation was made to roughly derive the movement of the particles in the solution. If magnetic force F is applied on magnetic particles, the equation of motion in solution is:

$$m \cdot \ddot{x} + \gamma \cdot \dot{x} = F \quad (2)$$

Where x is the particle displacement, m is the particle mass and γ is the damping coefficient. The drag force is linear with speed and in the sphere case is given by Stokes' law [33]:

$$F_{\text{drag}} = 6 \cdot \pi \cdot \eta \cdot r \cdot v = \gamma \cdot \dot{x} \quad (3)$$

Where η is the water viscosity ($\eta = 8.9 \cdot 10^{-4} \text{ Pa} \cdot \text{sec}$), r is the particle radius and v is the particle velocity. The magnetic force varies as a function of the magnetic particle position inside the borosilicate glass cuvette due to changes in the magnetic field gradient. For parabolic shaped pole tip, the variation of the field gradient is [20,31]:

$$\frac{\partial B}{\partial r} = \frac{4 \cdot \mu_0 \cdot M_s \cdot \beta}{(4 \cdot \beta \cdot (z_0 - x) + 1)^2} \quad (4)$$

Where β defines the parabolic curvature of the pole tip, $\mu_0 = 4\pi \cdot 10^{-7} \text{ N} \cdot \text{A}^{-2}$ is the vacuum permeability, M_s is the saturation magnetization of the pole material, z_0 is the distance from the pole tip to the center of the cuvette and x is the particle position inside the cuvette relative to the center of the cuvette (see Fig. (4a)). The variation of the field gradient inside the cuvette while the current was $I = 1.4 \text{ A}$ (which applied magnetization of $\mu_0 M_s = 0.7 \text{ Tesla}$ [20]) and the distance from the parabolic shaped pole tip to the center of the cuvette was $z_0 = 2 \text{ mm}$ is presented in Fig. (4b). Assuming the cuvette's inner dimension width was $500 \mu\text{m}$, x varied from $-250 \mu\text{m}$ to $+250 \mu\text{m}$.

Inserting equations (4) and (3) into equation (2), one can derive the particles equation of motion in water:

$$\bar{m}_B \cdot \frac{4 \cdot \mu_0 \cdot M_s \cdot \beta}{(4 \cdot \beta \cdot (z_0 - x) + 1)^2} - 6 \cdot \pi \cdot \eta \cdot r \cdot \dot{x} = m \cdot \ddot{x} \quad (5)$$

Using equation (5) we estimated the minimal displacement of a single magnetic bead that is located at the far end from the pole (particles that are located closer to the pole will feel much higher magnetic field and therefore will gain more distance during the same period of time).

As can be seen in Fig. (5), using the current set up and beads, at frequencies higher than 3 Hz, a single bead cannot be maneuvered from side to side more than $100 \mu\text{m}$. Moreover, although the current in the opposite solenoid is reduced to zero during the off period of the inactive pole, there is always some remanence in the inactive pole which applies negative force on the particle and further limiting the displacement of the beads.

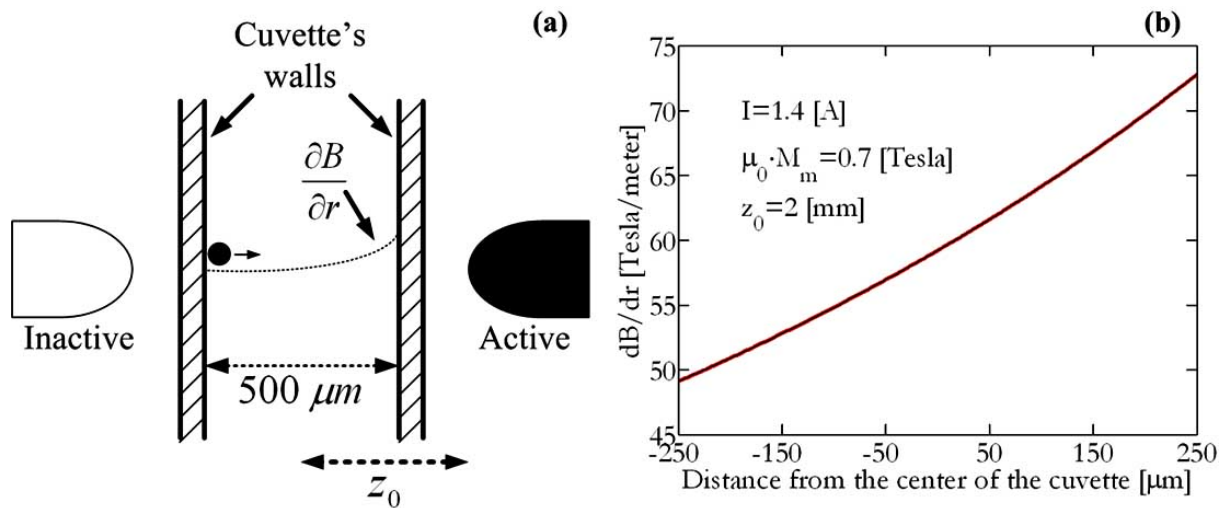


Fig. (4). (a) magnetic poles configuration. Dotted line shows the expected magnetic field gradient (b) calculated magnetic field gradient deviation inside the borosilicate glass cuvette (applied by the right pole).

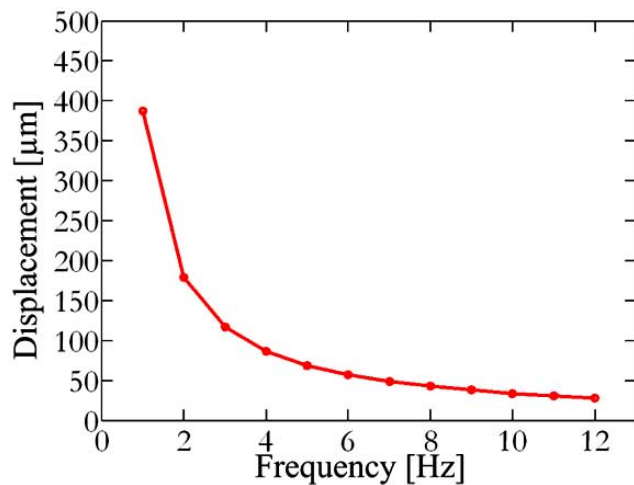


Fig. (5). Single bead displacement at different frequencies (simulation parameters identical to those of Fig. (4)).

The total force which is applied on a single magnetic particle drops rapidly and reaches minimum within $\sim 1\text{-}2 \mu\text{s}$ (see Fig. (6a)). Nevertheless, once the magnetic fields gradient is applied successively to the beads, a condensation phase begins until most of the beads are condensed, aggregated and maneuvered in a 1-D motion between the poles. The condensation phase stimulates the aggregation of the beads. Once two or more beads are gathered together, the aggregated beads mass and magnetic moment increase (linear with the number of aggregated beads). The magnetic force which is linear with the number of aggregated beads increases. However, the drag force is linear with the surface area of the aggregated beads and therefore increases much less than the magnetic force. Hence, the initial total force increases and drops to minimum less rapidly (e.g. the total power that is applied on 10,000 beads drops to minimum only within 1-2 ms, see Fig. (6b)). Such increase in the total force acting on the aggregated magnetic particles enables them to be maneuvered from side to side inside the cuvette in a periodic 1-D movement.

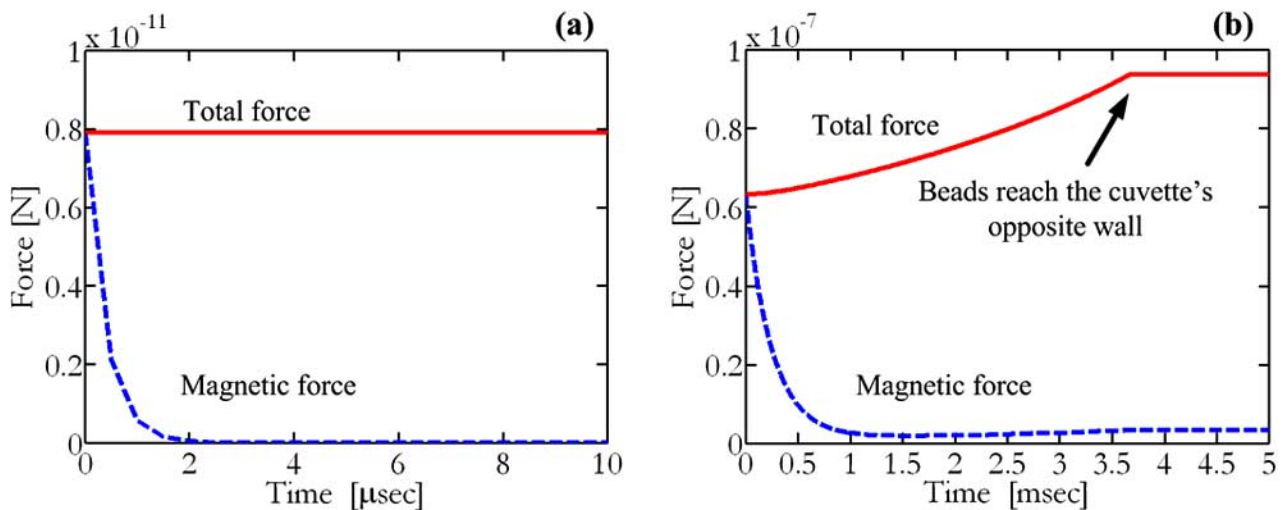


Fig. (6). Theoretical calculation of the magnetic and total (magnetic and drug) force that is applied on (a) a single bead (b) 10,000 beads (Dynabeads, M-280, Invitrogen).

There are two aspects that should be considered when choosing magnetic beads for the MMB system. The beads should have minimum auto-fluorescence in the detection wavelength and they should be superparamagnetic in order to allow manipulation in a periodic motion. For example, silica-based magnetic beads (SiMAG-streptavidin, Chemcell) exhibited less auto fluorescence than polystyrene-based magnetic beads (Dynabeads, M-280, Invitrogen). However, these beads are not superparamagnetic and therefore, after the removal of the magnetic field gradient they still pose some remanence. As a result, the beads showed much more self aggregation and could not be used in the MMB system.

4. DETECTION OF FLUORESCENT-LABELED PROBES AT SUB PICOMOLAR CONCENTRATIONS

We first tested the system capability to detect low concentration of fluorescent-labeled DNA probes (without quenching and without any target DNA) [20]. A 17bp DNA probe, which was labeled with AlexaFluor488 and biotin on the same nucleotide at the 5' end, was sequentially diluted in Tris-HCl buffer. In order to verify the affinity between the fluorescent-labeled oligos and the streptavidin-coupled magnetic beads we mixed magnetic beads (Dynabeads, M-280, Invitrogen) with different concentration of oligos. We received different amount of fluorescent-labeled oligos per bead for each solution. The emission from 10 to 30 beads from each solution was examined using a laser scanning microscope (LSM-510-META, Zeiss). As can be seen in Fig. (8), for $\sim 1 \cdot 10^2$ probes per bead the signal is too weak and is not higher than the auto fluorescence of the naked beads. However, for $\sim 1 \cdot 10^3$ probes per bead the signal is 3.2 higher than the signal from a naked bead. It should also be noted that the negative charge of the fluorescent-labeled oligos turns the beads into negative particles. Thus, in order to allow aggregation of the beads, low ratio of fluorescent-labeled oligos per bead should be kept.

We generated two series of solutions. The "test series" was prepared by mixing different amount of magnetic beads (Dynabeads, M-280, Invitrogen) with different concentrations of fluorescent-labeled oligos in 75 μ L volume cuvette (0.5 x 5.0 mm I.D., RT4905, Vitrocom). The average fluo-

rescent-labeled oligos per bead was kept to be approximately $1 \cdot 10^3$. The final fluorescent-labeled oligos' concentrations were 5, 2.5, 1.25, 0.625 and 0.5 pM. The "reference series" was prepared by mixing the same amount of magnetic beads with Tris-HCl buffer (without any fluorescent dye). In order to allow detection at lower concentrations we enlarged the solution volume to 270 μ L (0.4 x 8.0 mm I.D., RT2548, Vitrocom) and added 3 more solutions at final fluorescent-labeled oligos' concentrations of 0.5, 0.25 and 0.1 pM. The solutions were examined using the MMB system [20].

In all concentrations, the signal of the "test solution" (marked in red) was between 2-8 times higher than the "reference solution" (marked in black). At the lowest oligos concentration of 0.1 pM, the detected signal was 3.3 times higher than the noise, thereby implying detection sensitivity of 30 fM for a signal to noise ratio of 1. The main noise source in the system was the auto fluorescent light emitted from the beads. Higher volume resulted with higher number of beads for the same concentrations. Therefore, the higher noise level and signal level seen in Fig. (7b). In Summary, the MMB system showed the ability to aggregate as little as $12 \cdot 10^3$ beads (with 2.8 μ m diameter) in solution and to detect approximately $\sim 1 \cdot 10^3$ fluorescent-labeled probes per bead.

5. RAPID DETECTION OF SEQUENCES CODING FOR THE IBARAKI VIRUS COMPARED TO RT-PCR AND LASER SCANNING MICROSCOPE

While it was shown earlier that the magnetic modulation biosensing technique has very promising potential in specific DNA sequences detection, up until now only fluorescent labeled probes have been detected. Here we show how it may be employed for biological detection. To this end, we have chosen to detect, by this method, the NS3, non structural protein of the Ibaraki virus.

We generated two short DNA probes. A 19bp DNA probe ("quenched probe") was labeled with AlexaFluor488 and biotin on the same nucleotide at the 5' end and with a dark quencher (BHQ1) at the 3' end. A 17bp DNA probe ("unquenched reference probe") was labeled with only AlexaFluor488 and biotin on the same nucleotide at the 5' end.

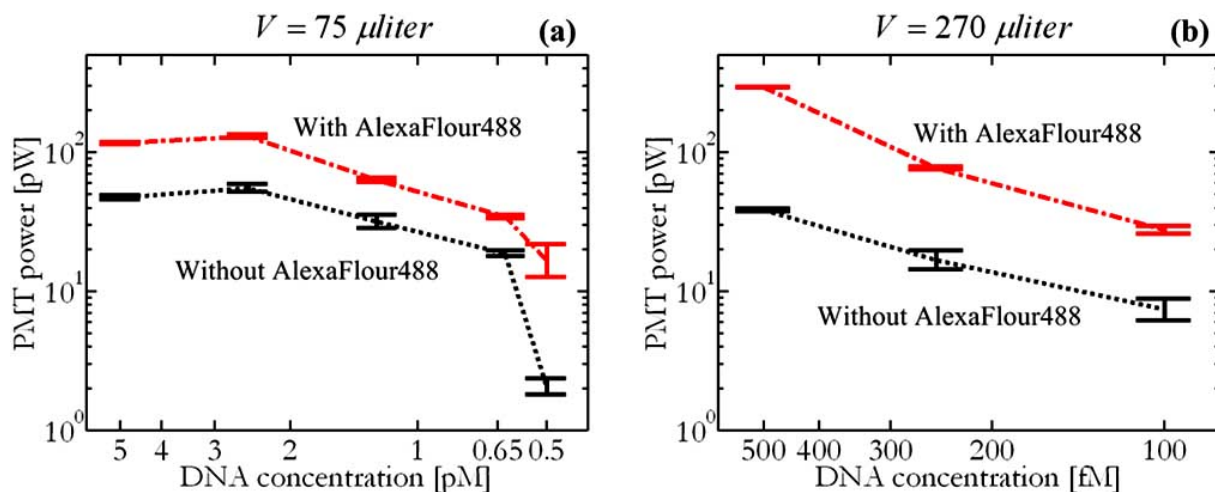


Fig. (7). The photomultiplier output power as a function of the fluorescent-labeled oligos concentrations (a) using a 75 μ L cuvette (b) using a 270 μ L cuvette.

The unquenched reference probe served as a top limit to the maximum fluorescent emission from a cleaved probe (assuming 100% cleavage activity during *Taq* polymerase reaction). The assay background noise (assuming no target is detected) was expected to be the residual fluorescent emission from biotinylated quenched probes bound to streptavidin-coupled magnetic beads (Dynabeads, M-280, Invitrogen). This residual emission was evaluated using a laser scanning microscope. The average fluorescent emission of the quenched probes and the unquenched reference probes for different amount of probes per bead is compared in Fig. 8). For the same amount of probes per bead the fluorescent residual emission of the quenched probe is much smaller than that of an unquenched reference probe. The signal to noise ratio between the unquenched reference probes to the quenched probes using the laser scanning microscope was estimated to be between 2 to 6.

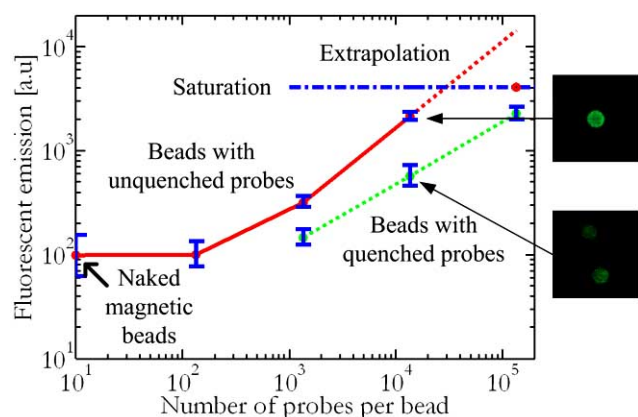


Fig. (8). Average fluorescent emission of streptavidin-coupled magnetic beads (Dynabeads, M-280, Invitrogen) attached to unquenched reference probes and to quenched probes, for different amount of probes per bead.

MMB sensitivity and detection time were evaluated using different number of PCR amplification cycles, namely 18 cycles, 10 cycles, 5 cycles, 3 cycles, and a single cycle. PCR amplifications were carried out in 20 μ l final volume with 150 pg of the Ibaraki Virus NS3 cDNA ligated into pEGFP-N1 vector ($\sim 2.3 \cdot 10^7$ copies) as our target. In order to identify the minimum amount of probe needed for detection, different concentrations of the quenched probe were added to each reaction according to the number of cycles. Control reactions were prepared the same way excluding the addition of the target. After PCR amplification, each experiment (with and without the target) was mixed with $20 \cdot 10^3$ (low number of cycles) to $440 \cdot 10^3$ magnetic beads (high number of cycles) and examined using the MMB system and a laser scanning microscope. When using MMB, for each reaction, the beads aggregated within approximately 30 s and the lock-in amplifier output voltage was measured for 25-50 s. The MMB system could clearly distinguish the target from control after 3 cycles and even after only a single cycle (see Fig. 9b). For comparison, the laser scanning microscope detected significant increase in the average fluorescent emission from the beads only after 18 amplification cycles [21]. For the same amount of initial DNA target (150 pg in 20 μ l) the fluorescent signal detected by RT-PCR was significant (above background level) only after 12.4 cycles (see Fig. 9a).

The results verified the feasibility of the novel FRET-based MMB assay presented here. The 5'-3' exonuclease activity of the *Taq* polymerase cleaved the fluorescent label from the probe while keeping it and the biotin still connected to the ribose. Thus, the cleaved fluorescent dye could be attached to the streptavidin coupled beads and produce light. On the other hand, in the control reaction, the probe remained intact and the fluorescent dye remained quenched by the dark quencher. The MMB system detected 1.9 pM of the Ibaraki Virus NS3 cDNA ($\sim 2.3 \cdot 10^7$ copies in 20 μ l) after a

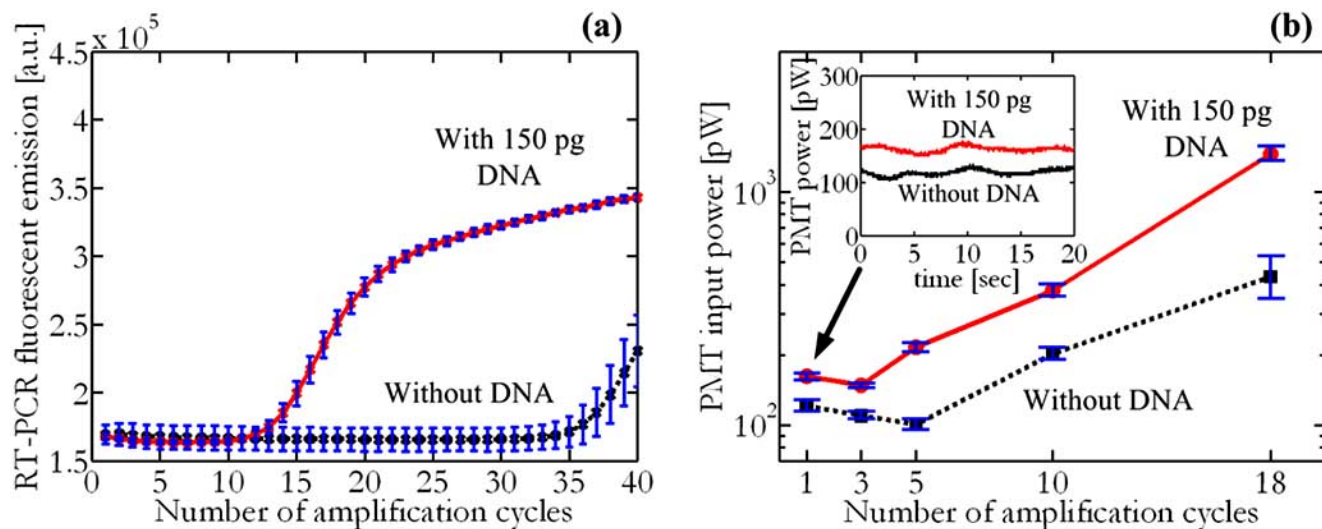


Fig. (9). (a) Real time PCR fluorescence as a function of PCR amplification cycles with initial 150 pg target DNA (red curve) and without DNA (black curve) (b) average PMT input power in the MMB system as a function of PCR amplification cycles (solid red line – with initial 150 pg target DNA, black dashed line – without DNA). Inset: Time trace of PMT input power after a single PCR cycle with 150 pg target DNA (solid red line) and without DNA (dashed black line).

single cycle of PCR (~18 min) without any washing or separation step. Further optimization of the single PCR cycle can reduce this time to approximately ~5 min. Moreover, one of the advantages of MMB is its ability to detect low concentrations at higher volumes due to the magnetic condensation. Thus, enlarging the volume from 20 μL used here (owing to the thermal cycler constraints) to 270 μL (full capacity of the current cuvette) should allow sensitivity of 140 fM.

6. HOMOGENEOUS DETECTION OF PROTEINS AT LOW CONCENTRATIONS USING 'SANDWICH'-BASED ASSAY

One of the main sources of background noise using the FRET-based MMB assay was the residual fluorescent emission from the quenched probes. The residual fluorescence from the quenched probe can be eliminated using a three-component 'sandwich' assay, in which the magnetic beads are coupled to the fluorescent label only via the target (i.e. 'sandwich'-based assay). A common commercially available heterogeneous immunoassay to detect angiogenesis biomarkers is provided by Bio-Rad laboratories (Bio-Plex[®] Precision Pro[™] [34]). In Bio-Plex[®] assay, a capture antibody directed against the desired target cytokine is covalently coupled to magnetic beads. The coupled beads are allowed to react with the sample containing the target cytokine. After a series of washes to remove unbound protein, a biotinylated detection antibody specific for a different epitope is added to the reaction. The result is the formation of a sandwich of antibodies around the target cytokine. Streptavidin-phycoerythrin (streptavidin-PE) is then added to bind to the biotinylated detection antibodies [35]. After an additional washing step the contents of the well are drawn up into a flow-based microplate reader system. The fluorescent signal from approximately 100 beads is averaged and reports the level of target protein in the well. The magnetic beads in this system allow magnetic washing instead of vacuum filtration. Thus, automation of several washing steps is made possible. Nevertheless, using this assay one cannot avoid at least four washing and separation steps which complicate the procedure [35]. However, using the MMB system, due to modulation of the magnetic beads, only the modulated fluorescent signal is detected by the lock-in amplifier. When the target cytokine doesn't exist in the solution, the beads will not be attached to the fluorescent protein and no signal will be generated. The modulation separates the beads from the background noise of the fluorescent protein and therefore eliminates the need for any washing and separation step. We present here preliminary results of human interleukin-8 (IL-8) detection using the MMB system.

The 'sandwich'-based IL-8 assay is illustrated in Fig. (10) and is based on Bio-Plex[®] Precision Pro[™] cytokine assays [34,35]. The reaction mixture included $\sim 1 \cdot 10^3$ paramagnetic beads (8 μm diameter) with IL-8 capture antibody, 0.48 pg of recombinant human IL-8 target, biotinylated IL-8 antibody and streptavidin coupled fluorescent protein (streptavidin PE). The components were added successively to the assay buffer [35] and then were shaken for 30 minutes. A control reaction was prepared the same way without the IL-8 target. Both the control and the target were inspected using the MMB system without any separation or washing step. When the IL-8 target was present, both the

capture antibody and the biotinylated antibody attached to it. The streptavidin-coupled fluorescent proteins connected to the magnetic beads via the biotinylated antibodies. Each bead could be attached to millions of fluorescent proteins. Once the beads passed through the laser beam in a synchronous motion it produced an alternating fluorescent signal. Conversely, when the IL-8 target wasn't present, the magnetic beads couldn't be attached to the fluorescent protein and therefore, the beads' synchronous motion in and out the laser beam didn't generate any signal in the MMB system.

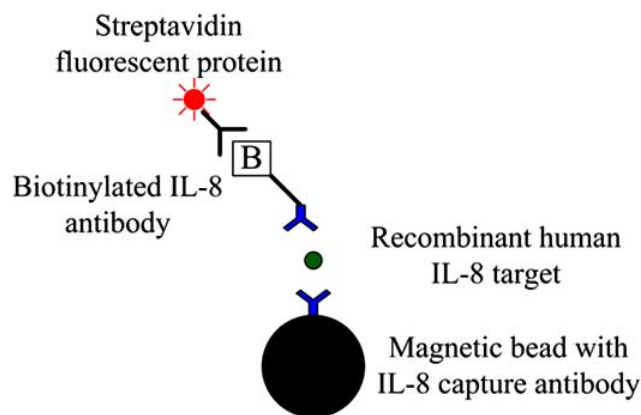


Fig. (10). Illustration of the 'sandwich'-based IL-8 assay: (a) magnetic beads with IL-8 capture antibody are added to the solution (b) When IL-8 target is present, both the capture antibody and the biotinylated antibody attach to the target (c) The streptavidin-coupled fluorescent proteins are connected via the biotin to the magnetic beads. (d) Each magnetic bead can be attached to millions of fluorescent proteins and set in 1-D periodic motion.

The pole modulation clock (yellow) and the PMT output signal (magenta) while detecting 0.48 pg IL-8 target are presented in Fig. (11). The modulation frequency for each pole was set at 2 Hz. However, as it was theoretically expected (see Fig. (3)), when the beads pass the laser beam, the PMT detects the fluorescent light and there is a peak in the PMT output voltage (the peak appears negative due to the PMT amplifier). Therefore, the demodulation frequency is at 4 Hz. When the PMT signal and the doubled-modulation clock (at

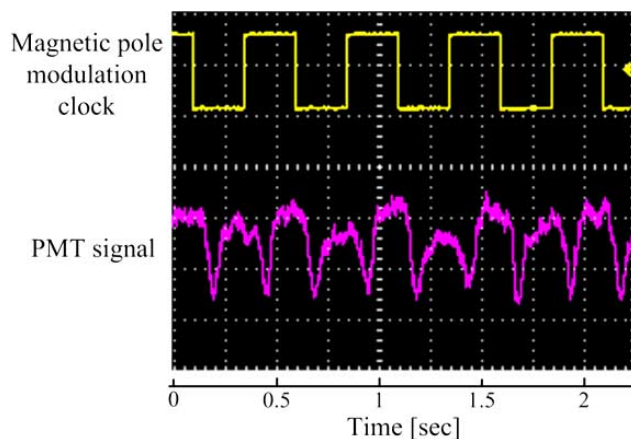


Fig. (11). The magnetic pole modulation clock (top white square wave) and the PMT signal (bottom signal) when detecting 0.48 pg IL-8 target.

4 Hz) are fed to the lock in amplifier, the sensitive phase detector detects the synchronization and results with high voltage (approximately 700mV). However, when the control sample was tested, the lock in amplifier didn't detect any signal (i.e. no locking). Thus, the MMB system can be used to detect rapidly and sensitively the presence of IL-8 without any washing or separation step. Future work should put emphasis on quantitative measurements of the IL-8 target.

7. CONCLUSIONS

In conclusion, the aim of the research was to develop a new approach for rapid, simple and sensitive detection of a target in homogeneous solution. As a first step, we have shown that magnetic modulation and synchronous detection can be utilized to rapidly detect small concentrations of fluorescent-labeled DNA probes. The modulated motion of the fluorescent dye in and out of the orthogonal laser beam produces a periodic signal at the PMT. The effect of modulation shifts the signal from DC to the modulation frequency, reduces the 1/f noise and separates the signal from the background residual scattering. The MMB system provides results within seconds after aggregation and avoids washing steps, typically incorporated in most heterogeneous assays. We demonstrated that there is a very promising potential to the MMB technique by reaching detection sensitivity of 30 fM of fluorescent labeled oligonucleotides (oligos).

As a second step, we have shown that MMB can be used for the rapid and sensitive detection of the Ibaraki virus NS3 gene ligated into pEGFP-N1. The novel FRET-based assay discriminated between the target DNA and the control, without DNA. The reaction time (~18 minutes), the sensitivity (1.9pM) and simplicity (homogeneous solution, no washing steps) suggest that the MMB system can be implemented in the field for rapid detection of pathogens. The MMB system provided faster results than real time PCR due to condensation and modulation of the beads. The real time PCR required 12 amplification stages to detect the fluorescent signal. In comparison, MMB is simple, provides immediate average of thousands of beads and allows elimination of background noise from the non-magnetized solution due to modulation. A single cycle was sufficient for detecting the signal in the MMB system. The system can be further improved in the future by optimization of the single *Taq* Polymerase activity cycle to shorten the reaction time, and by enlarging the detection volume to allow detection at the femtomolar level.

As a third step we demonstrated the MMB system capability to detect proteins (rather than DNA) while using a 'sandwich'-based assay (rather than a FRET-based assay). The preliminary results showed detection sensitivity of 0.48 pg IL-8 target.

Translocation and modulation of the fluorescent dye attached to DNA probe can also be done using an external electric field rather than a magnetic field, thereby taking advantage of the nucleotides electric charge. In this case, the solution in which the assay is performed should be without ions to avoid the presence of currents through the sample and non-specific modulation. Moreover, as some fluorophores are very sensitive to the pH, modulation of the signal can also be achieved by periodically changing the solution pH.

Nevertheless, one of the advantages of magnetic modulation is the condensation of most of magnetic beads in a small area, where the laser beam is focused. Hence, lower concentrations can be detected by simply increasing the solution volume.

Further improvements of the fluorescent signal can be achieved by using fluorescent nanoparticles (quantum dots) or by adding anti photo-bleaching reagents. Improvements in the instrumental photon detection efficiency can increase the average photon yield per molecule as well.

In addition to biosensing, the techniques that were developed in this work for external manipulation and condensation of particles may be used for other applications. For example, magnetically-coupled therapeutic compounds can be manipulated *in vivo* using magnetic fields generated outside the body. The magnetic field gradients are focused on the specific targets *in vivo*, capture the particle complex and enhance drug delivery to the target site [36]. Magnetic modulation and synchronous detection can also be used to enhance the contrast for *in vivo* imaging applications (see for example Aaron *et al.* (2006) [23], Wei *et al.* (2009) [37]).

ACKNOWLEDGEMENTS

The authors wish to thank the Ishaya Horwitz Fund for financial support, Dr. Alex Barbul, Dr. Konstantin Bogdanov, Dr. Nihay Laham-Karam, and Dr. Ofir Riss, for their assistance in the measurements and for fruitful discussions.

REFERENCES

- [1] Yeh, H.C.; Chao, S. Y.; Ho, Y.P.; Wang, T.H. Single-molecule detection and probe strategies for rapid and ultrasensitive genomic detection. *Curr. Pharm. Biotechnol.*, **2005**, *6*, 453-461.
- [2] Easterday, W. R.; Van Ert, M. N.; Zaneckim S.; Keim, P. Specific detection of *Bacillus anthracis* using TaqMan mismatch amplification mutation assay. *Biotechniques*, **2005**, *38*, 731-735.
- [3] Foutlier, B.; Moreno-Hagelsieb, L.; Flandre, D.; Remacle, J. Comparison of DNA detection methods using nanoparticles and silver enhancement. *IEE Proc. Nanobiotechnol.*, **2005**, *152*(1), 3-12.
- [4] Willner, I.; Katz, E., Eds.; *Bioelectronics: From Theory to Applications*; Wiley-VCH: Weinheim, **2005**.
- [5] Moerner, W. E.; Frommm, D. P. Methods of single-molecule fluorescence spectroscopy and microscopy. *Rev. Sci. Instrum.*, **2003**, *74*(8), 3597-3619.
- [6] Barnes, M. D.; Whitten, W. B.; Ramsey J. M. Detecting single molecules in liquids. *Anal. Chem.*, **1995**, *67*, 418A-423A.
- [7] Ivnitski, D.; Abdel-Hamid, I.; Atanasov, P.; Wilkins, E. Biosensors for detection of pathogenic bacteria. *Biosens. Bioelectron.*, **1999**, *14*, 599-624.
- [8] Alsmadi, O. A.; Bornarth, C. J.; Song, W.; Wisniewski, M.; Du, J.; Brockman, J. P.; Faruqi, A. F.; Hosono, S.; Sun, Z.; Du, Y.; Wu, X.; Egholm, M.; Abarzua, P.; Laskon, R. S.; Driscoll, M. D. High accuracy genotyping directly from genomic DNA using rolling circle amplification based assay. *BMC Genomics*, **2003**, *4*, 21.
- [9] Hall, J. G.; Eis, P. S.; Law, S. M.; Reynaldo, L. P.; Prudent, J. R.; Marshall, D. J.; Allawi, H. T.; Mast, A. L.; Dehlberg, J. E.; Kwiatkowski, R. W.; de Arruda, M.; Neri, B. P.; Lyamichev, V. I. Sensitive detection of DNA polymorphisms by the serial invasive signal amplification reaction. *Proc. Natl. Acad. Sci. USA*, **2000**, *97*, 8272-8277.
- [10] Castro, A.; Williams, J. G. K. Single-molecule detection of specific nucleic acid sequences in unamplified genomic DNA. *Anal. Chem.*, **1997**, *69*, 3915-3920.
- [11] Wabuyele, M. B.; Farquar, H.; Stryjewski, W.; Hammer, R. P.; Soper, S. A.; Cheng, Y.; Barany F. Approaching real-time molecular diagnostics: single-pair fluorescence resonance transfer

- (spFRET) detection for the analysis of low abundant point mutation in K-ras Oncogenes. *J. Am. Chem. Soc.*, **2003**, *125*, 6937-6945.
- [12] Foldes-Papp, Z.; Kinjo, M.; Tamura, M.; Birch-Hirschfeld, E.; Demel, U.; Titz G. P. A new ultrasensitive way to circumvent PCR-based allele distinction: Direct probing of *unamplified* genomic DNA by solution-phase hybridization using two-color fluorescence cross-correlation spectroscopy. *Exp. Mol. Pathol.*, **2005**, *78*, 177-189.
- [13] Park, S. J.; Taton, T. A.; Mirkin C. A. Array-based electrical detection of DNA with nanoparticle probes. *Science*, **2002**, *295*, 1503-1506.
- [14] Storhoff, J. J.; Lucas, A. D.; Garimella, V.; Bao, Y. P.; Muller, U. R. Homogeneous detection of unamplified genomic DNA sequences based on colorimetric scatter of gold nanoparticle probes. *Nat. Biotechnol.*, **2004**, *22*, 883-887.
- [15] Bao, Y. P.; Huber, M.; Wei, T. F.; Marla, S. S.; Storhoff, J. J.; Muller, U. R. SNP identification in unamplified human genomic DNA with gold nanoparticle probes. *Nucleic Acids Res.*, **2005**, *33*, e15.
- [16] Nam, J. M.; Stoeva, S. I.; Mirkin, C. A. Bio-bar-code-based DNA detection with PCR-like sensitivity. *J. Am. Chem. Soc.*, **2004**, *126*, 5932-5933.
- [17] Tanaka, S.; Aspanut, Z.; Kurita, H.; Toriyabe, C.; Hatsukade, Y.; Katsura, S. A DNA detection system based upon a high T_c SQUID and ultra-small magnetic nanoparticles. *IEEE Trans. Appl. Supercond.*, **2005**, *15*, 664-667.
- [18] Yeh, H. C.; Ho, Y. P.; Shih, L. M.; Wang T. H. Homogeneous point mutation detection by quantum dot-mediated two-color fluorescence coincidence analysis. *Nucleic Acids Res.*, **2006**, *34*, e35.
- [19] Zhang, C. Y.; Yeh, H. C.; Kuroki, M. T.; Wang T. H. Single quantum dot based DNA nanosensor. *Nat. Mater.*, **2005**, *4*, 826-831.
- [20] Danielli, A.; Arie, A.; Porat, N.; Ehrlich, M. Detection of fluorescent-labeled probes at sub-picomolar concentrations by magnetic modulation. *Opt. Express.*, **2008**, *16*, 19253-19259.
- [21] Danielli, A.; Porat, N.; Arie, A.; Ehrlich, M. Rapid homogenous detection of the Ibaraki virus NS3 cDNA at pico-molar concentrations by magnetic modulation. *Biosens. Bioelectron.*, **2009**, *25*, 858-863.
- [22] Pankhurst, Q. A.; Connolly, J.; Jones, S. K.; Dobson J. Applications of magnetic nanoparticles in biomedicine. *J. Phys. D Appl. Phys.*, **2003**, *36*, R167-R181.
- [23] Aaron, J. S.; Oh, J.; Larson, T. A.; Kumar, S.; Milner, T. E.; Sokolov, K. V. Increased optical contrast in imaging of epidermal growth factor receptor using magnetically actuated hybrid gold/iron oxide nanoparticles. *Opt. Express.*, **2006**, *14*, 12930-12943.
- [24] Anker, J. N.; Kopelman, R. Magnetically modulated optical nanoprobe. *Appl. Phys. Lett.*, **2003**, *82*, 1102-1104.
- [25] Anker, J. N.; Behrend, C. J.; Huang, H.; Kopelman, R. Magnetically-modulated optical nanoprobe (MagMOONs) and systems. *J. Magn. Magn. Mater.*, **2005**, *293*, 655-662.
- [26] Anker, J. A.; Behrend, C. J.; Kopelman, R. Aspherical magnetically modulated optical nanoprobe (MagMOONs). *J. Appl. Phys.*, **2003**, *93*, 6698-6700.
- [27] Morrison, L. E. Homogeneous detection of specific DNA sequences by fluorescence quenching and energy transfer. *J. Fluorescence*, **1999**, *9*, 187-196.
- [28] Willner, I.; Baron, R.; Willner, B. Integrated nanoparticle-biomolecule systems for biosensing and bioelectronics. *Biosens. Bioelectron.*, **2007**, *22*, 1841-1852.
- [29] McChlery, S. M.; Clarke, S. C. The use of hydrolysis and hairpin probes in real-time PCR. *Mol. Biotechnol.*, **2003**, *25*, 267-274.
- [30] Tanase, M.; Biais, N.; Sheetz, M. Magnetic tweezers in cell biology. *Method. Cell Biol.*, **2007**, *83*, 473-493.
- [31] de Vries, A. H. B.; Krenn, B. E.; van Driel, R.; Kanger, J. S. Micro magnetic tweezers for nanomanipulation inside live cells. *Biophys. J.*, **2005**, *88*, 2137-2144.
- [32] Private communication with Technical Services, Dynal Bead Based Separations, Invitrogen Group, Invitrogen Dynal AS, Isreal, **2008**.
- [33] Owen, J. P.; Ryu, W. S. The effects of linear and quadratic drag on falling spheres: an undergraduate laboratory. *Eur. J. Phys.*, **2005**, *26*, 1085-1091.
- [34] Bio-Plex Pro™, Bio-Rad "Human angiogenesis assay panel", <http://www.cancer.dartmouth.edu/shared/Documents/HumanAngiogenesisKit.pdf>. version: 10010584 US/EG Rev A Sig 1106.
- [35] Bio-Plex® Precision Pro™ Cytokine Assay, Instruction Manual, Bio-Rad Laboratories, Hercules, CA. version: 10008318 US/EG Rev A 06-0143 0305 Sig 1106
- [36] Dobson, J. Magnetic nanoparticles for drug delivery. *Drug Dev. Res.*, **2006**, *67*, 55-60.
- [37] Wei, Q.; Song, H. M.; Leonov, A. P.; Hale, J. A.; Oh, D.; Ong, Q. K.; Ritchie, K.; Wei, A. Gyromagnetic Imaging: Dynamic optical contrast using gold nanostars with magnetic cores. *J. Am. Chem. Soc.*, **2009**, *131*, 9728-9734.